2023 20th International Conference on Ubiquitous Robots (UR)
June 25-28, 2023. Hawaii Convention Center, Honolulu, Hawaii

Vision and Olfactory-based Wildfire Monitoring with Uncrewed Aircraft Systems

Lingxiao Wang[1], Shuo Pang[2], Mantasha Noyela[3], Kevin Adkins[4], Lulu Sun[5], and Marwa El-Sayed[6]

***Abstract*— Wildfires threaten human lives, destroy facilities, and emit toxic smoke. Traditional wildfire monitoring methods are hindered by inflexibility (e.g., watch towers) and cannot provide precise geo-location of wildfires (e.g., satellites). Thanks to recent development in robotics, deploying uncrewed aircraft systems (UAS) to monitor wildfires has become a feasible solution. This article introduces a UAS-based wildfire monitoring system and implement it in a prescribed burn test. A multirotor UAS was employed as the search agent and carried both olfactory (i.e., carbon monoxide and particulate matter) and visual (i.e., a camera) sensors to detect the existence of wildfires. A fuzzy inference system is designed to fuse olfactory sensor outputs to estimate whether the UAS detects smoke. A deep learning model, i.e., You Only Look Once version 4 (YOLOv4), is employed to identify smoke from the captured images. We deployed the proposed UAS in a prescribed burn at Tallahassee, Florida, in May 2022. Experimental results show that the proposed fuzzy inference system improves the estimation accuracy of whether the UAS detects smoke compared with the fixed threshold algorithm. In addition, the proposed YOLOv4 model can also detect smoke from captured images with a small amount of training samples.**

I. Introduction

Forests and grasslands play numerous critical economic and ecologic roles in nature. Forests stabilize and fertilize soil, purify water and air, store carbon, moderate climate, and sustain plant and animal biodiversity. However, with the increasing frequency and severity of extreme weather due to climate change, the occurrence of wildfires has increased, causing heavy death tolls and devastating destruction [1]. As an example, in Northern California, a wildfire, known as the "Camp Fire", ended up killing 85 people, burning 153,336 acres, and destroying 18,733 structures in 2018 [2].

To prevent large-scale wildfires, the most effective action is to detect fires in an early stage and provide information to firefighters for faster containment and suppression [3]. Traditional wildfire detection methods include human patrols, smoke detectors, thermal sensors, watch towers, satellite imagery, and manned aircraft [4]. However, these methods have limitations in practical applications. For instance, smoke and thermal sensors are point detectors that cannot provide information on the exact location or the size of the fire; human patrols are affected by complex terrain and fatigue; watch towers are constrained with a limited field of view, lack of flexibility, and high false alarm rate; satellite observations involve many tradeoffs and no satellite that is currently in orbit was specifically designed for rapid fire detection.

(a) (b)

Fig. 1. Deploying a UAS with both vision and olfaction sensors in a prescribed burn to monitor wildfires. (a) The UAS is ready to take off and (b) the UAS is flying above the burning area to collect air quality and meteorological data. These images were taken from the prescribed burn conducted in May 2022.

With the recent developments in robotics and autonomous systems, uncrewed aircraft systems (UAS) have been proposed as a more convenient and flexible technology for wildfire detection and observation [5]. Characterized by rapid maneuverability, the ability to see over a long range, and high personnel safety, UAS with suitable sensory modules have great potential for wildfire monitoring and detection tasks. In comparison to manned aircraft, UAS can access high-risk zones to provide an over-the-hill view and perform night time missions without putting human lives at risk [6]. Moreover, multirotor UAS can hover over a fixed position to monitor fire behavior and provide a continuous video stream for firefighters to plan optimal suppression strategies. The advantages that UAS afford can help overcome many of the limitations of traditional fire monitoring methods and offer a significant contribution in early detection and suppression of wildfires.

Existing UAS-based wildfire monitoring systems usually use visual detection devices, e.g., cameras, to observe wildfires. Compared to visual signals, the olfactory signal (i.e., the sense of smell) is more instructive in sensing the existence of wildfires from a long distance. Chemical/smoke plumes emitted from wildfire can travel several kilometers

[1]Lingxiao Wang is with Electrical Engineering Department, Louisiana Tech University, Ruston, LA 71272, USA lwang@latech.edu
[2]Shuo Pang is with Electrical Engineering and Computer Science Department, Embry-Riddle Aeronautical University, Daytona Beach, FL 32114, USA shuo.pang@erau.edu
[3]Mantasha Noyele is with Computer Science Department, Louisiana Tech University, Ruston, LA 71272, USA man032@latech.edu
[4]Kevin Adkins is with Aeronautical Science Department, Embry-Riddle Aeronautical University, Daytona Beach, FL 32114, USA kevin.adkins@erau.edu
[5]Lulu Sun is with Engineering Fundamentals Department, Embry-Riddle Aeronautical University, Daytona Beach, FL 32114, USA lulu.sun@erau.edu
[6]Marwa El-Sayed is with Civil Engineering Department, Embry-Riddle Aeronautical University, Daytona Beach, FL 32114, USA Marwas.ElSayed@erau.edu

2023 20th International Conference on Ubiquitous Robots (UR) | 979-8-3503-3517-0/23/$31.00 ©2023 IEEE | DOI: 10.1109/UR57808.2023.10202419

with the wind advection, and these plumes can be detected with chemical/smoke sensors [7]. Further, unlike visual signals, smoke plumes will disperse in the air regardless of obstacles and can also be detected at night time, where visual signals are usually blocked by obstacles and are impacted by darkness.

Motivated by this consideration, we installed both olfactory and visual sensors on a multirotor UAS to detect wildfires. Olfactory sensors, including a particulate matter (PM) and a carbon monoxide (CO) sensor, were employed to detect PM and CO gas, which are two main materials in the emitted smoke [8]. The visual sensor was an onboard camera, which can capture 4K images and videos to monitor wildfire. Fig. 1 presents the employed UAS with the sensor suite installed. Besides, we designed two data-processing algorithms to process olfactory and visual sensor data to identify the existence of wildfire. Specifically, a fuzzy inference system was devised to fuse CO and PM sensor readings to estimate whether the UAS detects smoke, and a deep learning model, i.e., YOLOv4, was implemented to recognize smoke from captured images. In May 2022, we deployed the proposed UAS in a prescribed burn in Tallahassee, Florida. Through this experiment, we found that the proposed UAS is feasible for detecting and monitoring wildfires, and the selected olfactory sensors can correctly identify smoke detection and non-detection events. These preliminary results helped us design more advanced odor plume tracing navigation algorithms.

II. Background

A. The Use of UAS in Wildfire Monitoring Operations

The use of UAS for wildfire monitoring started in 1996. A fixed-wing aircraft, named Firebird, was employed to aid firefighters in Montana, U.S. [9]. Firebird was equipped with a TV and an onboard infrared camera, enabled it to capture fire images from an over-the-hill view. A few years later, NASA Ames Research Center (NASA-ARC) and the United States Forest Services (USFS) conducted the First Response Experiment (FiRE) project using a fixed-wing UAS, ALTUS II, carried a thermal scanner to construct the fire images [10]. Another large scale project called COMETS, funded by the European Commission, started research on the coordination of multiple UAS for wildfire monitoring [11], [12]. During the period of 2005-2009, the USFS and NASA-ARC conducted a series of prescribed burns to demonstrate the utility of small UAS on wildfire monitoring by capturing wildfire images [9]. Apart from the U.S., various UAS-based wildfire monitoring experiments were conducted in Europe, including [13]–[15].

Existing UAS-based wildfire monitoring systems center on using vision based systems (i.e., images captured from visual or infrared cameras) to detect wildfires. The use of other robotic sensing abilities, such as olfaction, is rare in recently published wildfire detection systems. Moreover, most of these projects, e.g., [16]–[20], solve the research problems in the phase of active fire monitoring, e.g., designing a coordination algorithm to organize UAS to detect wildfire perimeters.

B. Vision-based Wildfire Monitor Systems

Current vision-based wildfire monitor systems use remote camera networks to detect wildfires [21], such as the High Performance Wireless Research & Education Network [22], ALERT wildfire camera [23], and ForestWatch [24]. The vision-based wildfire detection system has a very high false alarm rate. In California, local fire agencies have previously deployed at least one vision-based automated smoke detection system, ForestWatch from EnviroVision, but these deployments were abandoned because the systems were plagued by high false detection rates [25]. An evaluation of ForestWatch in Canada [26] documents an initial false positive rate of more than 300 per day, that was reduced to 10–30 per day even after fine-tuning camera settings. Another problem is that the vision-based detection accuracy is affected significantly by weather (e.g., mist, cloud, fog, etc.), light conditions (e.g., night time), picture angles, etc.

Compared to stationary cameras, it is more preferable to employ UAS (equipped with cameras) to detect wildfires. Due to the high maneuverability of UAS, wildfire images can be captured from different angles and at a close distance. With the rapid development of artificial intelligence and machine learning techniques, deep learning methods are commonly-used in identifying fires from images captured from vision-based UAS wildfire monitoring systems [27]. For instance, Zhang et al. [28] presented a saliency detection method to fast locate and segment core fire areas from aerial images, where a 15-layered self-learning convolutional neural network (CNN) was devised to process images to detect fires. Alexandrove et al. [29] implemented three deep learning-based object detection algorithms to detect smoke in the aerial images.

C. Robotic Olfaction

Robotic olfaction enables robots to detect odor plumes in environments. This technology can be used to find odor sources in hazardous environments [30]. The most commonly-used robotic platform in robotic olfaction is a ground mobile robot. For instance, Li *et al.* [31] employed a ground vehicle to find an ethanol source in an outdoor environment. Pang *et al.* [32] implemented the artificial potential field (APF) algorithm on a Pioneer 3 ground robot to find an odor source. Robotic olfaction can also be applied in underwater environments to find underwater odor sources. Li *et al.* [33] proposed an autonomous underwater vehicle (AUV) based application to find underwater hydrothermal vents.

On flying robots, Gao *et al.* [34] presented a multirotor UAS-based application to find an odor source in an indoor environment. In Eu and Yap's work [35], a quadrotor drone is controlled to vary its height to search odor plumes. Luo *et al.* [36] presented a flying odor compass to detect odor plumes in a three dimensional space. Aurell *et al.* [37] presented a UAS-based smoke sampling platform that carried different

TABLE I

SPECIFICATION OF THE EMPLOYED MULTIROTOR UAS

Weight	6.27 lbs
Max Speed	49 mph
Max Flight Time	18 mins
Max Takeoff Weight	7.71 lbs

TABLE II

SPECIFICATIONS OF ONBOARD VISUAL AND OLFACTORY SENSORS. L×W×H: LENGTH×WIDTH×HEIGHT.

	Name	Dimension (L×W×H, Inches)	Weight (Ounces)	Measurements
Visual Sensor	Zenmuse X3 4K Camera	4×3×1	3	4K Videos and Images
Olfactory Sensors	CO-B4	1×1×0.6	0.4	Carbon Monoxide
	OPC-N3	3×2.4×2.5	2.7	PM1, PM2.5, PM10

gas sensors to measure air quality data such as nitric oxide (NO) and nitrogen dixoide (NO2). The US Environmental Protection Agency (EPA) conducted a trial, where a UAS was employed to sample air quality data over a prescribed burn site [38]. The research niche of this work is to implement both olfactory and visual sensors on a UAS. Both sensors are utilized to detect existence of wildfires via CO/PM detection and image-processing techniques to recognize smokes from captured images.

III. METHODOLOGY

A. UAS Hardware and Onboard Sensors

In this project, we employed a flexible multirotor UAS (Inspire 1, DJI Inc.) as the robotic agent to detect and monitor wildfires. The specification of this UAS is presented in Table I. We attached a 4K camera (Zenmuse X3, DJI Inc.) as the visual sensor to capture wildfire images. For olfactory sensors, we installed a CO (CO-B4, Alphasense Inc.) and particulate matter (PM) sensor (OPC-N3, Alphasense Inc.) to detect CO and PM concentrations. Table II shows the specifications of the visual and olfactory sensors.

As shown in Fig. 2(a), the camera is attached at the bottom of the UAS with a 3-axis gimbal, which enables the camera to capture images in ± 320 degrees in the horizontal plane and -90 to $+30$ degrees in the pitch direction. Olfactory sensors are installed on a 3-D printed shelf, which is rigidly attached on the front of the UAS for better air intake. Fig. 2(b) presents the configuration of sensors, microprocessor, and transmission modules. Olfactory sensors and the wireless transmission module are connected to an onboard Arduino Uno, which will send sensor readings back to a computer in the ground station via a wireless transmission link. On the other hand, the onboard camera will send live videos back to a remote controller on the ground station. Therefore, we can monitor live olfactory sensor readings and videos captured from the UAS on the ground. The wireless data transmission link between the Arduino and the ground station is at 413 MHz, and the video transmission link is at 2.4

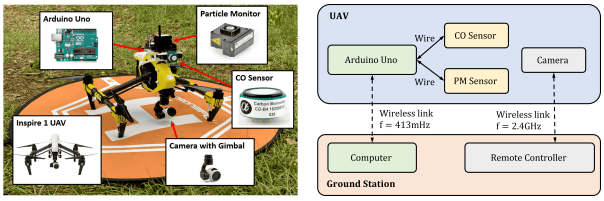

(a) (b)

Fig. 2. The UAS and onboard sensors. (a) The Inspire 1 UAS and the installed sensory modules. (b) The configuration of sensors, transmission modules, and the onboard microprocessor.

GHz. Thus, the frequency inference does not exist. Maximal transmission distance for the video transmission is 5.1 miles, and for olfactory data transmission, the maximal distance is 1 mile. The updating frequency of olfactory sensors is 1 Hz.

B. Data Process of Olfactory Sensor Measurements

In this project, two olfactory sensors, including a CO and a PM sensor, are employed to detect smokes. An important characteristic for the employed CO sensor is that it has a quick response time and a long recovery time [39]. In other words, the measurements rises quickly when the CO sensor is exposed to the CO gas and drops slowly when the sensor is away from CO gas. By contrast, the employed PM sensor has an opposite characteristic: its recovery time is very short but the response time is not as rapid as the CO sensor. Therefore, the goal was to design a data fusion algorithm that combines the benefits from two olfactory sensors and use it to estimate whether the UAS detects smokes.

The challenge in this task is how to effectively combine two sources of information (i.e., CO and PM readings) to accurately estimate smoke detection. Due to the unknown features of the sensor response models and the testing environment, we designed a fuzzy inference system to fuse two sensor readings and calculate a probability of the UAS detecting smoke. In fuzzy theory, vague variables and environments can be handled via linguistic descriptions and rules. Therefore, by analyzing sensor measurements, we can estimate the current detection and non-detection event. A fuzzy inference system contains three parts, including fuzzification, fuzzy rules, and defuzzification [40].

1) Fuzzification: Fuzzification is the step that changes real values of inputs and outputs into fuzzy values, which are the degree of uncertainty that real values belong in a fuzzy set.

The simplest way to define fuzzy inputs is using the original CO and PM sensor measurements directly. However, both CO and PM sensors have recovery time, meaning that the original sensor measurements cannot accurately reflect whether the UAS detects smoke or not. By analyzing sensor measurements of the employed olfactory sensors, we found that the gradient of sensor measurements is more reliable and instructive in distinguishing smoke detection and non-detection events. For instance, if the gradient is negative, it is very likely that the UAS leaves and does not detect the smoke even though the current sensor measurement is high (the sensor could be in the recovery time). On the other hand,

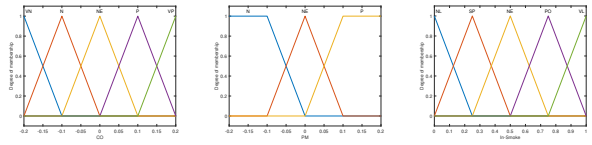

(a) (b) (c)

Fig. 3. Membership functions and fuzzy sets for inputs and output. (a) CO gradient (b) PM gradient (c) $P_{detection}$.

if the gradient is positive, it is very likely that the UAS enters and detects the smoke. Therefore, we define inputs of the proposed fuzzy inference system as the gradient of CO and PM sensor measurements. The output of the fuzzy inference system is a probability (denoted as $P_{detection}$), representing the likelihood of the UAS detecting smokes.

The gradient of sensor measurements can be calculated by the following equations. Denote $x(t)$ as the sensor measurement at t, the gradient $G(t)$ at t can be calculated as [41]:

$$G(t) = \begin{cases} 0 & t = 0 \\ x(t) - x(t-1) & t > 0 \end{cases}, \tag{1}$$

Additionally, all sensor data is normalized (between 0 to 1) before the calculation to eliminate the effect of different sensor output units.

Fig. 3 shows fuzzy membership functions for inputs and the output. Since we found that the CO gradient was more varying than the PM gradient in the collected data, we defined five fuzzy membership functions for CO gradient and three for the PM gradient. For the output, we defined five fuzzy membership functions. All membership functions are triangular functions. Specifically, the first input, i.e., CO gradient, has five membership functions, including VN (very negative), N (negative), NE (neutral), P (positive), and VP (very position). The second input, i.e., PM gradient, has three membership functions, including N, NE, and P. For the output, i.e., the probability of detecting smokes, there are five membership functions, including NL (not likely), SP (slightly possible), NE (neutral), PO (possible), and VL (very likely).

2) Fuzzy Rules: Fuzzy rules are determined based on the sensor characteristics. As mentioned, the employed CO sensor has a long recovery time and a short response time, while the PM sensor has a short recovery time and a long response time. Thus, the rise in CO measurements is more reliable in indicating smoke detection, and the drop in PM measurements is more effective to reflecting the smoke non-detection. In terms of gradients, if the gradient of CO measurements is positive, i.e., the CO reading increases, it is very likely that the UAS detects smoke. On the other hand, if the PM gradient is negative, i.e., the PM reading decreases, there is a high chance that the UAS does not detect smoke. According to the above analysis, two sample fuzzy rules can be defined in a 'IF-THEN' format:

IF CO gradient is VP AND PM gradient is N, THEN $P_{detection}$ is VL.

TABLE III

LIST OF FUZZY RULES. VN: VERY NEGATIVE; N: NEGATIVE; NE: NEUTRAL; P: POSITIVE; VP: VERY POSITIVE; NL: NOT LIKELY; SP: SLIGHTLY POSSIBLE; PO: POSSIBLE; VL: VERY LIKELY.

Rule No.	Inputs		Output
	CO Gradient	PM Gradient	$P_{detection}$
1	VN	N	NL
2	VN	NE	NL
3	VN	P	SP
4	N	N	NL
5	N	NE	NL
6	N	P	NE
7	NE	N	NL
8	NE	NE	NE
9	NE	P	PO
10	P	N	SP
11	P	NE	PO
12	P	P	VL
13	VP	N	NE
14	VP	NE	VL
15	VP	P	VL

IF CO gradient is N AND PM gradient is N, THEN $P_{detection}$ is NL.

Table III enumerates all possible combinations of inputs and outputs and presents fifteen fuzzy rules (in a 'IF-THEN' format) in the proposed fuzzy controller.

3) Defuzzification: Defuzzification is a procedure that maps the fuzzy output to a crisp signal. In this work, the centroid method [42] is selected as the defuzzification algorithm, which can be expressed as follow:

$$P_{detection} = \frac{\sum_{i=1}^{n} Q_i \cdot \mu(Q_i)}{\sum_{i=1}^{n} \mu(Q_i)}, \tag{2}$$

where $P_{detection}$ is the probability of detecting smokes; i is the index of fuzzy rules, i.e., $i \in [1, 15]$; Q_i denotes the center of the active membership function of the output variable provided by the ith rule; $\mu(Q_i)$ is the output of the conjunction degree of the IF part of the ith rule.

C. Image Processing of Visual Sensor Data

In this work, the image processing algorithm is to detect and extract smoke areas from the captured images in real-time. This visual detection provides direct insight regarding the existence of wildfires. Recent years, using deep learning techniques in image processing is ubiquitous, and there are many pre-trained deep learning models for image processing tasks. Employing a pre-trained model is more efficient than devising and training a new deep learning model from scratch since the pre-trained model needs fewer training images to reach a high detection accuracy [43]. Here, we employed a pre-trained deep learning model, i.e., You Only Look Once Version 4 (YOLOv4) [44], to detect smoke from images and videos. In this section, we introduce the YOLOv4 architecture, training datasets, and the testing results after the training.

1) The YOLOv4 Model: The YOLOv4 [44] is an object detection model that is used to detect different objects from images or videos. When objects are found in images, these

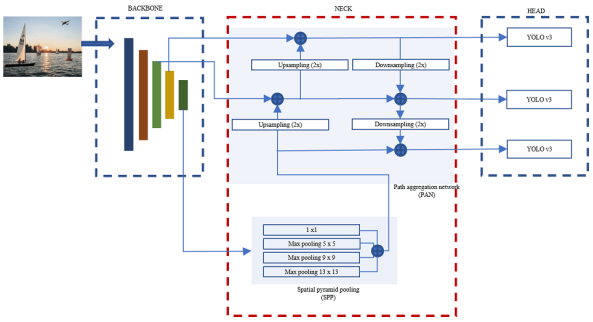

Fig. 4. The YOLOv4 architecture. From left to right, three components are the backbone, neck, and head, respectively. In this work, the backbone is selected as a pre-trained CNN, named CSPDarknet53; the neck connects the backbone and heads; three heads are YOLOv3 networks that predict the bounding boxes, classification scores, and objectiveness scores, respectively. This image was retrieved from [45].

object classes are enclosed in a bounding box and their class is identified. YOLOv4 is a one-stage object detector that uses a single network to detect object region and classify the object.

Fig. 4 presents the implemented YOLOv4 model's architecture, which contains three components, namely backbone, neck, and head. The backbone is typically a pre-trained convolutional neural network (CNN) on a large image dataset, e.g., ImageNet. It is responsible for extracting features from images for later classification. In this work, the backbone is selected as the CSPDarknet53 network, which is a combination of Darknet53 and the Cross Stage Partial (CSP) networks [46]. The Darknet53 is a 53 layers deep CNN, and the CSP network is a special network architecture that splits the feature map into two parts and sends one copy through the dense block and sends the other straight on to the next stage. The neck connects the backbone and the head, which concentrates features extracted from the backbone and sends them to the head for classification. In the head, categorization and localization information are estimated. For the implemented YOLOv4 model, it has has three detection heads, and each head is a YOLOv3 network that predicts the bounding boxes, classification scores, and objectiveness scores, respectively.

2) Training Data: Training data is imperative to the DL model's performance. A diverse dataset allows the DL model to train general rules in object detection, improving the detection accuracy. In this project, we used Wildfire Smoke Image dataset [47] to train the selected DL model. As shown in Fig. 5, the dataset contains various smoke images from different views, which were collected from remote wildfire monitoring cameras [22]. This dataset contains 737 smoke images, of which 516 were used for training and 221 for testing.

3) Training Process: We downloaded the training dataset to train the YOLOv4 model for up to 6,000 iterations in order to achieve accurate classification and localization. Each thousand steps in our suggested technique produced a trained weight file. Using this weight file, we computed the values of four information measures based on the testing dataset while

(a) (b)

Fig. 5. Sample smoke images retrieved from the Wildfire Smoke Image dataset [48].

Fig. 6. Prediction result of the YOLOv4 after the training. We can see that the YOLOv4 model can correctly detect and label smoke in images.

keeping the 0.25 and 0.50 confidence threshold values. The six weight files we obtained in this way were stored, and the most effective ones were eventually applied to smoke detection. The values of the information measures calculated to evaluate the best-trained weight files are shown. The average map value of our model is 94 percent, which is excellent for smoke detection. A sample testing image is presented in Fig. 6, where the smoke areas are correctly detected. Our model processed each image in the testing data set on average in 77 milliseconds on the computer with an Intel i9-12900 CPU and a Nvidia RTX 3090 GPU. When processing live or recorded video, we reached a frame rate of 14 frames per second.

IV. Experiment

A. Prescribed Burn Field and the Flight Trajectory

In May 2022, we collaborated with the Tall Timber fire institution to conduct a prescribed burn at Tallahassee, Florida. Fig. 7(a) shows the satellite image of the prescribed burning area. The size of the burn area is approximately 9 acres, which is a forest land inside the Tall Timber fire institution. In the spring season, the Tall Timber fire institution conducts a prescribed burn to eliminate weeds and fertilize the land.

During the prescribed burn, we deployed a multirotor UAS and successfully collected data during the burn. In the flight, the UAS started at the downwind area of the burning region and flew upwind toward the burning region. The UAS was remotely controlled by a human operator, and the sensor data was transmitted to the ground station for live monitoring of the wildfires. Fig. 7(b) presents the trajectories of the flight, which was recorded from the onboard GPS. We can see that the UAS crossed the burning areas multiple times to collect the environmental data. The flight was conducted at the early phase of the prescribed burn, i.e., right after the ignition, and returned to the ground after around 15 minutes.

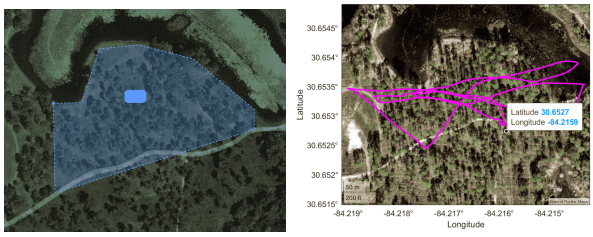

(a) (b)

Fig. 7. Deploying an UAS in a prescribed burn to collect environment data. (a) The prescribed burn area (highlighted with the blue color). (b) The flight trajectory of the UAS, where the UAS is controlled by the human operator. The labeled position in the diagram is the start position.

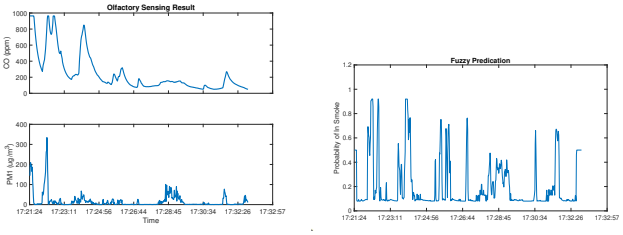

(a) (b)

Fig. 8. Recorded olfactory sensor measurements and outputs from the proposed fuzzy inference system. (a) The olfactory sensing data during the flight, including CO (the upper plot) and PM (the lower plot) data. (b) The data processing result of the proposed fuzzy inference system.

B. Recorded Sensor Data and Data Processing Results

Fig. 8 shows the plots of olfactory sensor readings in the flight and outputs from the proposed fuzzy inference system, which fuses CO and PM sensor reads to estimate whether the UAS detects smoke. Specifically, the upper diagram in Fig. 8(a) is the plot for recorded CO concentrations, and the lower diagram in Fig. 8(a) is the recorded PM concentrations. From these two plots, we can see that concentrations of CO and PM have similar changing trends throughout the flight. For instance, at 17:21:24, the UAS entered the smoke according to the video recording, and CO and PM concentrations were high simultaneously; at 17:22:15, the UAS left the smoke, and CO and PM concentrations were decreasing at the same time. In addition, we can clearly observe that the employed CO sensor has a quick response time and a slow recovery time, whereas the onboard PM sensor has a much quicker recovery time compared to the CO sensor.

Fig. 8(b) presents the output of the proposed fuzzy inference system, which is the probability of the UAS detecting smoke. We consider the UAS detects the smoke when the fuzzy output is larger than 0.1. Besides, by observing the recorded UAS videos, we can estimate and manually label the smoke detection and non-detection period. Therefore, we can compare the proposed fuzzy inference system, the gradient threshold algorithm, and the traditional fixed threshold algorithm in distinguishing the smoke detection and non-detection events. Fig. 9 presents the comparison result, where dotted lines represent the smoke detection periods.

There are six groups of data in Fig. 9, named as 'CO-

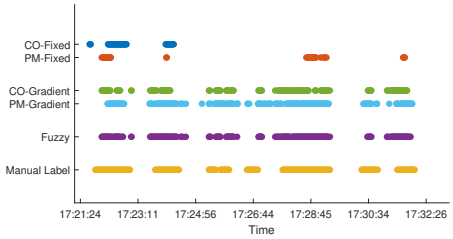

Fig. 9. The comparison of CO, PM, fuzzy inference system's output, and manual label from the recorded videos. The dotted line

Fixed', 'PM-Fixed', 'CO-Gradient', 'PM-Gradient', 'Fuzzy', and 'Manual Label'. Explanations of these labels are listed as follows. 1) 'CO-Fixed' and 'PM-Fixed' are results of the fixed threshold algorithm, which relies on a fixed threshold to distinguish smoke detection and non-detection events. For both CO and PM measurements, the threshold is defined as the average of first N recorded data when the UAS is not in smoke. $N = 100$ in this comparison. 2) 'CO-Gradient' and 'PM-Gradient' are results of the gradient threshold algorithm. If the gradient of CO or PM measurements is positive, we consider the UAS detects smoke; otherwise, the UAS does not detect smoke. Eqn. 1 is used to calculate the gradient for CO and PM. 3) 'Fuzzy' is the result from the proposed fuzzy inference method. We consider that the UAS detects the smoke when the fuzzy output is larger than 0.1; otherwise, the UAS does not detect smoke. 4) 'Manual Label' is the result from the manual labelling of recorded videos from the UAS's camera. From these videos, we can observe a complete process of the UAS entering and leaving smoke. In this comparison, we consider 'Manual Label' as the truth. The dotted lines shows the duration of smoke detection events.

From Fig. 9, we can observe that the proposed fuzzy inference system ('Fuzzy' in Fig. 9) has more overlaps with the 'Manual Label' data compared to the four other groups of data. Specifically, we can see that the fixed threshold algorithm cannot accurately recognize smoke detection and non-detection events since the overlapping periods between 'CO-Fixed'/'PM-Fixed' and 'Manual Label' are short. Besides, the gradient threshold algorithm is significantly better than the fixed threshold algorithm, where both 'CO-Gradient' and 'PM-Gradient' have more overlaps with 'Manual Label' compared to 'CO-Fixed' and 'PM-Fixed'. Comparing 'CO-Gradient'/'PM-Gradient' and 'Fuzzy', we can see that 'Fuzzy' is more reliable since it has more overlaps with 'Manual Label' than the other two plots, especially in 17:21:24 - 17:23:11 and 17:26:44 - 17:28:45. This result indicates that the proposed fuzzy inference system is more accurate in distinguishing smoke detection and non-detection events.

Finally, Fig. 10 demonstrates the smoke prediction results generated by the trained YOLOv4 model, where images were captured from the onboard camera during the prescribed burn. The time of images being captured are labeled beneath each diagram. From this group of images, we can see that the

(a) 17:22:36 (b) 17:22:37

(c) 17:26:33 (d) 17:26:39

(e) 17:26:42 (f) 17:27:37

Fig. 10. Smoke prediction generated by the trained YOLOv4 model. Images were captured from the UAS during the flight at different times. Red squares in the images highlighted the detected smoke areas. High resolution images can be found via this link [49].

YOLOv4 model can correctly label the smoke area from the captured images. We can also see the correlation between the olfactory and vision sensors. For instance, at 17:22:37 (i.e., Fig. 10(b)), the proposed YOLOv4 model detected the smoke from the image, the olfactory sensors simultaneously reported the smoke detection as we can see in Fig 9.

It is worth noting that the proposed YOLOv4 model is not very effective in detecting smoke near the UAS. For instance, as shown in Fig. 10(e) and (f), the proposed YOLOv4 model did not detect the smoke on the top side of the image, where the smoke is close to the UAS. This is because the training dataset only contains smoke images that were captured from remote watch towers, where the smoke position is far away from the camera. Due to this reason, we cannot conduct a comparison between YOLOv4 results and the 'Manual Label' data in Fig. 9 since 'Manual Label' indicates periods when the UAS is inside/outside the smoke.

C. Discussion and Future Works

1) The Limitations: As mentioned, the YOLOv4 model cannot detect smoke near the UAS effectively. The most straightforward method to overcome this problem is adding more training images containing smoke near the camera positions. Another limitation is the duration of UAS's operating time. In our experiment, the UAS could operate 20 mins per charge, and the communication distance is up to 1 mile. For full-scale wildfire localization task (e.g., finding a wildfire location from several kilometers away), a larger fixed-wing UAS with higher battery capacity should be employed as the search agent.

2) The Future Works: In the future, we can collect more training data to improve the performance of the YOLOv4 model. On the other hand, we could also combine image detection with olfactory sensing to produce the comprehensive detection that contains both near and far smoke. Since olfactory sensors rely on particle contact to detect smoke, they are ideal for detecting smoke near the UAS. Thus, the olfactory sensing data can serve as the complement of the vision detection to provide the comprehensive smoke information. This fused information could also be used to estimate smoke propagation areas and smoke source (i.e., wildfire) locations.

Fusing vision and olfaction signals to make reliable detection of wildfires (or smoke) is a promising research direction to pursue. Research [50] shows that olfaction and vision modalities are associated with human behaviors, where humans rely on the fusion of olfactory and visual signals to perceive the external world. Most UAS-based wildfire systems rely on vision-based instruments to detect wildfires. The integration of olfaction and vision is rare. In this work, the proposed CO and PM sensors and the fuzzy inference method show the capability of olfactory sensors in detecting smoke, which can be used as preliminary results for future researchers to integrate multiple perceptive abilities to produce a more reliable detection. In the future, we will consider fusing robotic olfaction and vision to produce comprehensive smoke information and use it to estimate smoke propagation areas and smoke source locations.

V. Conclusion

In this paper, we present a wildfire monitoring system using UAS. Besides using a camera to monitor wildfires, two olfactory sensors, including a CO and PM sensor, are added on the UAS to detect olfactory measurements. The proposed UAS system was implemented in a prescribed burn in Tallahassee, Florida. Experiment results show that both vision and olfactory sensors were instructive in detecting wildfires. Besides, the proposed fuzzy inference method is more reliable than the fixed threshold and gradient threshold algorithms in distinguishing smoke detection and non-detection events, and the proposed YOLOv4 model can detect smoke areas on the ground. Results presented in this work will help us and future researchers design autonomous odor plume tracing algorithms that combines both vision and olfaction.

References

[1] S. J. Hart, J. Henkelman, P. D. McLoughlin, S. E. Nielsen, A. Truchon-Savard, and J. F. Johnstone, "Examining forest resilience to changing fire frequency in a fire-prone region of boreal forest," *Global change biology*, vol. 25, no. 3, pp. 869–884, 2019.

[2] S. S. Schulze, E. C. Fischer, S. Hamideh, and H. Mahmoud, "Wildfire impacts on schools and hospitals following the 2018 california camp fire," *Natural Hazards*, vol. 104, no. 1, pp. 901–925, 2020.

[3] C. Kontoes, I. Keramitsoglou, N. Sifakis, and P. Konstantinidis, "Sithon: An airborne fire detection system compliant with operational tactical requirements," *Sensors*, vol. 9, no. 2, pp. 1204–1220, 2009.

[4] A. A. Alkhatib, "A review on forest fire detection techniques," *International Journal of Distributed Sensor Networks*, vol. 10, no. 3, p. 597368, 2014.

[5] F. A. Hossain, Y. Zhang, and C. Yuan, "A survey on forest fire monitoring using unmanned aerial vehicles," in *2019 3rd International Symposium on Autonomous Systems (ISAS)*, pp. 484–489, IEEE, 2019.

[6] C. R. Butler, M. B. O'Connor, and J. M. Lincoln, "Aviation-related wildland firefighter fatalities—united states, 2000–2013," *MMWR. Morbidity and mortality weekly report*, vol. 64, no. 29, p. 793, 2015.

[7] P. Intini, J. Wahlqvist, N. Wetterberg, and E. Ronchi, "Modelling the impact of wildfire smoke on driving speed," *International Journal of Disaster Risk Reduction*, vol. 80, p. 103211, 2022.

[8] S. R. Schneider, K. Lee, G. Santos, and J. P. Abbatt, "Air quality data approach for defining wildfire influence: Impacts on pm2. 5, no2, co, and o3 in western canadian cities," *Environmental Science & Technology*, vol. 55, no. 20, pp. 13709–13717, 2021.

[9] V. Ambrosia, T. Zajkowski, *et al.*, "Selection of appropriate class uas/sensors to support fire monitoring: experiences in the united states," in *Handbook of Unmanned Aerial Vehicles*, pp. 2723–2754, Springer, 2015.

[10] V. G. Ambrosia, S. S. Wegener, D. V. Sullivan, S. W. Buechel, S. E. Dunagan, J. A. Brass, J. Stoneburner, and S. M. Schoenung, "Demonstrating uav-acquired real-time thermal data over fires," *Photogrammetric engineering & remote sensing*, vol. 69, no. 4, pp. 391–402, 2003.

[11] A. Ollero, S. Lacroix, L. Merino, J. Gancet, J. Wiklund, V. Remuß, I. V. Perez, L. G. Gutiérrez, D. X. Viegas, M. A. G. Benitez, *et al.*, "Multiple eyes in the skies: architecture and perception issues in the comets unmanned air vehicles project," *IEEE robotics & automation magazine*, vol. 12, no. 2, pp. 46–57, 2005.

[12] L. Merino, J. R. Martínez-de Dios, and A. Ollero, "Cooperative unmanned aerial systems for fire detection, monitoring, and extinguishing," *Handbook of Unmanned Aerial Vehicles*, pp. 2693–2722, 2015.

[13] A. Restas, "Forest fire management supporting by uav based air reconnaissance results of szendro fire department, hungary," in *2006 First International Symposium on Environment Identities and Mediterranean Area*, pp. 73–77, IEEE, 2006.

[14] F. Esposito, G. Rufino, A. Moccia, P. Donnarumma, M. Esposito, and V. Magliulo, "An integrated electro-optical payload system for forest fires monitoring from airborne platform," in *2007 IEEE Aerospace Conference*, pp. 1–13, IEEE, 2007.

[15] M. Van Persie, A. Oostdijk, J. Fix, M. Van Sijl, and L. Edgardh, "Real-time uav based geospatial video integrated into the fire brigades crisis management gis system," *International archives of the photogrammetry, remote sensing and spatial information sciences*, vol. 38, no. 1, 2011.

[16] R. D. Ottmar, J. K. Hiers, B. W. Butler, C. B. Clements, M. B. Dickinson, A. T. Hudak, J. J. O'Brien, B. E. Potter, E. M. Rowell, T. M. Strand, *et al.*, "Measurements, datasets and preliminary results from the rxcadre project–2008, 2011 and 2012," *International Journal of Wildland Fire*, vol. 25, no. 1, pp. 1–9, 2016.

[17] K. Alexis, G. Nikolakopoulos, A. Tzes, and L. Dritsas, "Coordination of helicopter uavs for aerial forest-fire surveillance," in *Applications of intelligent control to engineering systems*, pp. 169–193, Springer, 2009.

[18] P. Sujit, D. Kingston, and R. Beard, "Cooperative forest fire monitoring using multiple uavs," in *2007 46th IEEE Conference on Decision and Control*, pp. 4875–4880, IEEE, 2007.

[19] F. Afghah, A. Razi, J. Chakareski, and J. Ashdown, "Wildfire monitoring in remote areas using autonomous unmanned aerial vehicles," in *IEEE INFOCOM 2019-IEEE Conference on Computer Communications Workshops (INFOCOM WKSHPS)*, pp. 835–840, IEEE, 2019.

[20] X. Hu, J. Bent, and J. Sun, "Wildfire monitoring with uneven importance using multiple unmanned aircraft systems," in *2019 International Conference on Unmanned Aircraft Systems (ICUAS)*, pp. 1270–1279, IEEE, 2019.

[21] F. Bu and M. S. Gharajeh, "Intelligent and vision-based fire detection systems: A survey," *Image and vision computing*, vol. 91, p. 103803, 2019.

[22] "Hpwren." `https://hpwren.ucsd.edu/cameras`.

[23] "Alertwildfire." `https://www.alertwildfire.org`.

[24] "Forestwatch." `http://evsusa.biz/productsservices/forestwatch`.

[25] K. Govil, M. L. Welch, J. T. Ball, and C. R. Pennypacker, "Preliminary results from a wildfire detection system using deep learning on remote camera images," *Remote Sensing*, vol. 12, no. 1, p. 166, 2020.

[26] D. Schroeder, *Operational trial of the forestwatch wildfire smoke detection system*. Forest Engineering Research Institute of Canada, 2005.

[27] A. Bouguettaya, H. Zarzour, A. M. Taberkit, and A. Kechida, "A review on early wildfire detection from unmanned aerial vehicles using deep learning-based computer vision algorithms," *Signal Processing*, vol. 190, p. 108309, 2022.

[28] Y. Zhao, J. Ma, X. Li, and J. Zhang, "Saliency detection and deep learning-based wildfire identification in uav imagery," *Sensors*, vol. 18, no. 3, p. 712, 2018.

[29] D. Alexandrov, E. Pertseva, I. Berman, I. Pantiukhin, and A. Kapitonov, "Analysis of machine learning methods for wildfire security monitoring with an unmanned aerial vehicles," in *2019 24th conference of open innovations association (FRUCT)*, pp. 3–9, IEEE, 2019.

[30] X. Chen and J. Huang, "Odor source localization algorithms on mobile robots: A review and future outlook," *Robotics and Autonomous Systems*, vol. 112, pp. 123–136, 2019.

[31] J. Li, Q. Meng, Y. Wang, and M. Zeng, "Odor source localization using a mobile robot in outdoor airflow environments with a particle filter algorithm," *Autonomous Robots*, vol. 30, no. 3, pp. 281–292, 2011.

[32] S. Pang and F. Zhu, "Reactive planning for olfactory-based mobile robots," in *2009 IEEE/RSJ International Conference on Intelligent Robots and Systems*, pp. 4375–4380, IEEE, 2009.

[33] W. Li, J. A. Farrell, S. Pang, and R. M. Arrieta, "Moth-inspired chemical plume tracing on an autonomous underwater vehicle," *IEEE Transactions on Robotics*, vol. 22, no. 2, pp. 292–307, 2006.

[34] B. Gao, H. Li, W. Li, and F. Sun, "3d moth-inspired chemical plume tracking and adaptive step control strategy," *Adaptive Behavior*, vol. 24, no. 1, pp. 52–65, 2016.

[35] K. S. Eu and K. M. Yap, "Chemical plume tracing: A three-dimensional technique for quadrotors by considering the altitude control of the robot in the casting stage," *International Journal of Advanced Robotic Systems*, vol. 15, no. 1, 2018.

[36] B. Luo, Q.-H. Meng, J.-Y. Wang, and M. Zeng, "A flying odor compass to autonomously locate the gas source," *IEEE Transactions on Instrumentation and Measurement*, vol. 67, no. 1, pp. 137–149, 2017.

[37] J. Aurell, B. Gullett, A. Holder, F. Kiros, W. Mitchell, A. Watts, and R. Ottmar, "Wildland fire emission sampling at fishlake national forest, utah using an unmanned aircraft system," *Atmospheric Environment*, vol. 247, p. 118193, 2021.

[38] "Tracking wildfire smoke: Epa researchers make better maps with drones." https://www.epa.gov/sciencematters/tracking-wildfire-smoke-epa-researchers-make-better-maps-drones.

[39] M. I. A. Asri, M. N. Hasan, M. R. A. Fuaad, Y. M. Yunos, and M. S. M. Ali, "Mems gas sensors: a review," *IEEE Sensors Journal*, 2021.

[40] L. A. Zadeh, "Fuzzy sets," *Information and control*, vol. 8, no. 3, pp. 338–353, 1965.

[41] S. C. Chapra, R. P. Canale, *et al.*, *Numerical methods for engineers*, vol. 1221. Mcgraw-hill New York, 2011.

[42] B. K. Bose, "Expert system, fuzzy logic, and neural network applications in power electronics and motion control," *Proceedings of the IEEE*, vol. 82, no. 8, pp. 1303–1323, 1994.

[43] S. J. Pan and Q. Yang, "A survey on transfer learning," *IEEE Transactions on knowledge and data engineering*, vol. 22, no. 10, pp. 1345–1359, 2009.

[44] A. Bochkovskiy, C.-Y. Wang, and H.-Y. M. Liao, "Yolov4: Optimal speed and accuracy of object detection," *arXiv preprint arXiv:2004.10934*, 2020.

[45] "Yolov4 in matlab." `https://www.mathworks.com/help/vision/ug/getting-started-with-yolo-v4.html`.

[46] C.-Y. Wang, H.-y. Liao, Y.-H. Wu, P.-Y. Chen, J.-W. Hsieh, and I.-H. Yeh, "Cspnet: A new backbone that can enhance learning capability of cnn," pp. 1571–1580, 06 2020.

[47] "Wildfire smoke dataset." https://universe.roboflow.com/brad-dwyer/wildfire-smoke.

[48] "Vott for image annotation and labeling." `https://blog.roboflow.com/vott/`.

[49] "High resolution images." `https://tinyurl.com/2fythapy`.

[50] S. Kuang and T. Zhang, "Smelling directions: olfaction modulates ambiguous visual motion perception," *Scientific reports*, vol. 4, no. 1, pp. 1–5, 2014.